

Event-by-event fluctuations in p+p and central A+A collisions within relativistic transport models

Anton Motornenko,^{1,2} Katarzyna Grebieszkow,³ Elena Bratkovskaya,^{2,4}
Mark I. Gorenstein,^{1,5} Marcus Bleicher,^{1,2,4} and Klaus Werner⁶

¹Frankfurt Institute for Advanced Studies, Giersch Science Center, Frankfurt am Main, Germany

²Institut für Theoretische Physik, Johann Wolfgang Goethe Universität, Frankfurt am Main, Germany

³Faculty of Physics, Warsaw University of Technology, Warsaw, Poland

⁴GSI Helmholtzzentrum für Schwerionenforschung GmbH, Darmstadt, Germany

⁵Bogolyubov Institute for Theoretical Physics, Kiev, Ukraine

⁶Laboratoire SUBATECH, University of Nantes - IN2P3/CNRS - Ecole des Mines, Nantes, France

(Dated: April 23, 2022)

Event-by-event multiplicity fluctuations in nucleus-nucleus collisions are studied within the relativistic transport models: EPOS, PHSD, and UrQMD. As measures of particle number fluctuations we consider the scaled variances $\omega[X]$ for positive, negative, and all charged hadrons, and the strongly intensive quantities $\Delta[K^+, \pi^+]$, $\Sigma[K^+, \pi^+]$ for K^+ and π^+ yields. At the SPS energy range the fluctuation measures are calculated for proton-proton, Ar+Sc, and Pb+Pb collisions. Comparison with recent NA61/SHINE and older NA49 measurements of the multiplicity fluctuations is done. The validity of the model of independent sources, and the role of experimental acceptance are studied.

PACS numbers: 24.10.Lx, 24.60.-k, 24.60.Ky, 25.495.-q

Keywords: nucleus-nucleus collisions, fluctuations, transport models, statistical models

I. INTRODUCTION

Fluctuations are expected to play an important role in study of the phase structure of QCD matter formed in relativistic heavy ion collisions [1–3]. The relativistic transport models such as EPOS[4, 5], PHSD [6, 7], and UrQMD [8, 9] allow to perform theoretical study of microscopical properties of systems that are created in nucleus-nucleus (A+A) collisions. This detailed description of A+A collisions allows to study the particle number fluctuations under different conditions, see, e.g., [10–16]. Recent data from the NA61/SHINE Collaboration [17] show a surprisingly different behavior of scaled variances ω for proton-proton (p+p) and A+A collisions. It is found that multiplicity fluctuations are much larger in p+p collisions than in most central A+A ones. This result is in contradiction with the wounded nucleon model. The aim of present work is to investigate the dependence of multiplicity fluctuations on system size and collision energy within the microscopical transport models.

II. EVENT-BY-EVENT FLUCTUATIONS IN TRANSPORT MODELS

In the present study the simulations of A+A collisions were performed within the transport models that were listed above. The calculations are done for systems of different size, i.e., p+p, Ar+Sc, and

Pb+Pb are studied. The collision energies are taken in a range of the CERN SPS accelerator which corresponds to the center of mass energy of nucleon pair $\sqrt{s_{NN}} = 5.1 \div 17.3$ GeV. All of the parameters of the present study are selected in a way to be as close as possible to the parameters of NA61/SHINE experiment (see, e.g., Refs. [18, 19]). Note, however, that in the aforementioned experiment the centrality selection is a rather complicated procedure defined by the number of projectile spectators [17, 20]. In our study, the centrality selection procedure is simplified: central A+A collisions are considered as those with zero impact parameter, $b = 0$ fm.

The following measures of particle number fluctuations are studied in the present work:

$$\omega[X] = \frac{\langle X^2 \rangle - \langle X \rangle^2}{\langle X \rangle}, \quad (1)$$

$$\Delta[A, B] = \frac{1}{C_\Delta} \left[\langle B \rangle \omega[A] - \langle A \rangle \omega[B] \right], \quad (2)$$

$$\Sigma[A, B] = \frac{1}{C_\Sigma} \left[\langle B \rangle \omega[A] + \langle A \rangle \omega[B] - 2(\langle AB \rangle - \langle A \rangle \langle B \rangle) \right], \quad (3)$$

$$C_\Delta = \langle A \rangle - \langle B \rangle, \quad C_\Sigma = \langle A \rangle + \langle B \rangle,$$

where X , A , and B denote the particle yields, and

$$\langle X \rangle = \frac{1}{N_{\text{ev}}} \sum_{i=1}^{N_{\text{ev}}} X_i \quad (4)$$

corresponds to the event-by-event averaging over a sample of N_{ev} events. The fluctuation measures (1-3) are intensive quantities, i.e., they do not depend on the system size. However, only Δ (2) and Σ (3), are called as strongly intensive quantities [21], because they are not sensitive to the fluctuations of the system volume. The system size event-by-event fluctuations in A+A collisions are usually a result of the varying impact parameter from collision to collision. Note that even at the fixed value of the impact parameter $b = 0$ the number of nucleon participants still fluctuates event-by-event, and these fluctuations influence the scaled variances $\omega[X]$.

In the present work the following goals are pursued:

- Study of particle number fluctuations versus collision energy and system size. Search for any non-monotonous behavior.
- Comparison of different transport models.
- Investigation of the role of different acceptance criteria.
- Comparison of $\omega[X]$, as a function of the system size, with the recent data of NA61/SHINE Collaboration.

There are two well known assumptions that connect the scaled variances obtained in different physical scenarios. The first one (see, e.g., [22]) predicts the value of $\omega_{\text{acc}}[X]$ in case some experimental acceptance (e.g., the kinematical acceptance in momentum space) is applied:

$$\omega_{\text{acc}}[X] = 1 - q + q\omega[X], \quad 0 < q = \frac{\langle X_{\text{acc}} \rangle}{\langle X \rangle} < 1, \quad (5)$$

where q is a ratio of the mean values of the accepted number of particles to the total one. Equation (5) ignores the correlations between accepted particles and predicts that at $q \rightarrow 0$ the scaled variance ω_{acc} *monotonously* goes to 1, the value that corresponds to the Poisson distribution.

The second assumption often used in A+A collisions is the model of independent sources, the so-called wounded nucleon model [23]. This model connects the scaled variance $\omega[X]$ of produced X -species particles in A+A collisions with the scaled variance $\omega_{\text{NN}}[X]$ and average multiplicity $\langle X \rangle_{\text{NN}}$ taken from nucleon-nucleon (NN) collisions at the same collision energy $\sqrt{s_{\text{NN}}}$:

$$\omega[X] = \omega_{\text{NN}}[X] + \omega_{\text{p}}[N_{\text{part}}] \frac{1}{2} \langle X \rangle_{\text{NN}}, \quad (6)$$

where $\omega_{\text{p}}[N_{\text{part}}]$ represents the scaled variance for the number of nucleon participants.

III. TRANSPORT MODELS

A. EPOS

Nucleus-nucleus scattering - even proton-proton - amounts to many elementary collisions happening in parallel. Such an elementary scattering corresponds to the exchange of a “parton ladder”.

A parton ladder represents parton evolution from the projectile and the target side towards the center (small x). The evolution is governed by an evolution equation, in the simplest case according to DGLAP. In the following we will refer to these partons as “ladder partons”, to be distinguished from “spectator partons” to be discussed later. It has been realized a long time ago that such a parton ladder may be considered as a quasi-longitudinal color field, a so-called “flux tube” [5], conveniently treated as a relativistic string. The intermediate gluons are treated as kink singularities in the language of relativistic strings, providing a transversely moving portion of the object. This flux tube decays via the production of quark-antiquark pairs, creating in this way fragments – which are identified as hadrons.

The technical details of the consistent quantum mechanical treatment of the multiple scattering with the energy sharing between the parallel scatterings can be found in [24]. Hard scale independent correction factors are added to the bare amplitude of the Pomeron to control the rise of the cross-section at high energy and the multiplicity in HI collisions. The treatment of these nonlinear effects at high energy is explained in [4].

All the results presented in this paper were obtained within the EPOS 1.99 model, however, the whole analysis was repeated also for EPOS LHC version and the results of fluctuation measures were found to be very close to the ones obtained in EPOS 1.99.

B. PHSD

The Parton-Hadron-String Dynamics (PHSD) transport approach [6, 7, 25, 26] is a microscopic covariant dynamical model for strongly interacting systems formulated on the basis of Kadanoff-Baym equations [26, 27]. The approach consistently describes the full evolution of a relativistic heavy-ion collision from the initial hard scatterings and string formation through the dynamical deconfinement phase transition to the strongly-interacting quark-gluon plasma (sQGP) as well as hadronization and the subsequent interactions in the expanding hadronic phase as in the Hadron-String-Dynamics (HSD) transport approach

[28]. The transport theoretical description of quarks and gluons in the PHSD is based on the Dynamical Quasi-Particle Model (DQPM) for partons that is constructed to reproduce lattice QCD for QGP thermodynamics [26, 30] via effective propagators for quarks and gluons. The PHSD differs from conventional Boltzmann approaches in following aspects:

- i) it incorporates dynamical quasi-particles due to the finite width of the spectral functions;
- ii) it involves scalar mean-fields that substantially drive the collective flow in the partonic phase;
- iii) it is based on a realistic equation of state from lattice QCD and thus describes the speed of sound $c_s(T)$ reliably;
- iv) the hadronization is described by the fusion of off-shell partons to off-shell hadronic states and does not violate the second law of thermodynamics;
- v) all conservation laws are fulfilled in the hadronization contrary to coalescence models;
- vi) the effective partonic cross sections are self-consistently determined within the DQPM and probed by transport coefficients in thermodynamic equilibrium (shear- and bulk viscosity, electric conductivity, magnetic susceptibility etc. [31, 35]).

In the beginning of relativistic heavy-ion collisions color-neutral strings (described by the LUND model [32]) are produced in highly energetic scatterings of nucleons from the impinging nuclei. These strings are dissolved into 'pre-hadrons'. If the local energy density is larger than the critical value for the phase transition, which is taken to be $\sim 0.5 \text{ GeV}/\text{fm}^3$, the pre-hadrons melt into (colored) effective quarks and antiquarks in their self-generated repulsive mean-field as defined by the DQPM [26, 30]. In the DQPM the quarks, antiquarks, and gluons are dressed quasi-particles and have temperature-dependent effective masses and widths which have been fitted to lattice thermal quantities such as energy density, pressure and entropy density.

The transition from the partonic to hadronic degrees-of-freedom is described by covariant transition rates for the fusion of quark-antiquark pairs to mesonic resonances or three quarks (antiquarks) to baryonic states. In the hadronic phase PHSD is equivalent to the hadron-strings dynamics (HSD) model [28, 29]. The PHSD approach has been applied to p+p, p+A and A+A collisions from lower SPS to LHC energies and been successful in describing of experimental data including single-particle spectra, collective flow as well as electromagnetic probes [7, 25, 33–36].

C. UrQMD

The UrQMD-model [8, 9] is a microscopic transport theory based on the covariant propagation of all hadrons on classical trajectories in combination with stochastic binary scatterings, color string formation and resonance decay. It represents a Monte Carlo solution of a large set of coupled partial integro-differential equations for the time evolution of the various phase space densities $f_i(x, p)$ of particle species $i = N, \Delta, \Lambda$, etc., which non-relativistically assumes the Boltzmann equation.

The exchange of electric and baryonic charge, strangeness and four-momentum in the t -channel is considered for baryon-baryon (BB) collisions at low energies, while meson-baryon (MB) and meson-meson (MM) interactions are treated via the formation and decay of resonances, i.e. the s -channel reactions. t -channel reactions for MB and MM collisions are taken into account from $\sqrt{s} > 3 \text{ GeV}$ on increasing to the only MB, MM interaction type above $\sqrt{s} = 6 \text{ GeV}$.

This framework allows bridging with one concise model the entire available range of energies from the SIS energy region ($\sqrt{s} \approx 2 \text{ GeV}$) to the RHIC energy ($\sqrt{s} = 200 \text{ GeV}$). At the highest energies, a huge number of different particle species can be produced. The model should allow for subsequent rescatterings. The collision term in the UrQMD model includes more than fifty baryon species and five meson nonets (45 mesons). In addition, their antiparticles have been implemented using charge-conjugation to assure full baryon-antibaryon symmetry.

All particles can be produced in hadron-hadron collisions and can interact further with each other. The different decay channels all nucleon-, Δ - and hyperon-resonances up to $2.25 \text{ GeV}/c^2$ mass as well as the meson (e.g. K^*) decays etc. are implemented. At higher energies the advantage of the hadron universality is taken and a string model for the decay of intermediate states is used.

IV. RESULTS

The simulations of A+A collisions are performed within the certain range of energies and system sizes: p+p collisions are studied at energies $\sqrt{s_{NN}} = 6.27, 7.75, 8.77, 12.33, 17.28 \text{ GeV}$, while for Ar+Sc and Pb+Pb collisions energies of the colliding system are $\sqrt{s_{NN}} = 6.12, 7.62, 8.77, 11.94, 16.84 \text{ GeV}$. These are the energies that are available in the NA61/SHINE experiment. The simulations of Ar+Sc and Pb+Pb collisions are performed with zero impact parameter ($b = 0 \text{ fm}$).

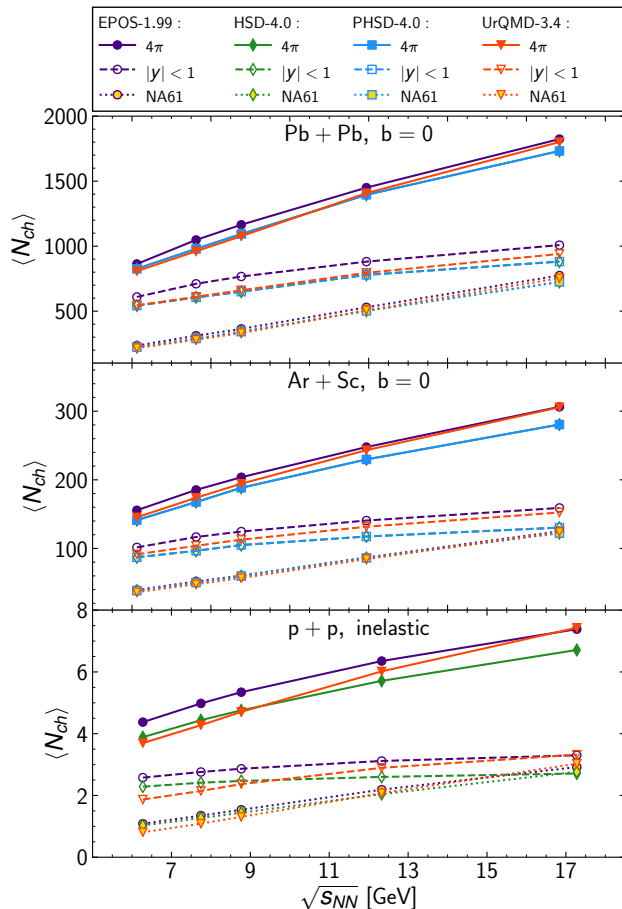


Figure 1: Comparison of average multiplicities of charged particles $\langle N_{ch} \rangle$ as functions of $\sqrt{s_{NN}}$ in $b = 0$ fm Pb+Pb (top), $b = 0$ fm Ar+Sc (middle), and inelastic p+p (bottom) collisions in EPOS-1.99, HSD-4.0, PHSD-4.0, and UrQMD-3.4 models.

Different acceptance cuts are applied for the transport model simulations. The results are presented in three different acceptance regions:

- full rapidity (4π) – all particles are considered in results;
- $|y| < 1$ acceptance – only particles with rapidity $-1 < y < 1$ in the center of mass frame are considered for calculation of measured quantities;
- the NA61/SHINE acceptance – where detector acceptance is applied, only pions π , kaons K , protons p and their antiparticles are taken into account (in experiment, most of other particles are rejected by a list of track cuts), and rapidity $0 < y < y_{\text{beam}}$ simultaneously with $p_T < 1.5$ GeV/c cuts are imposed. Finally, so-called

NA61/SHINE acceptance map [37] is applied in order to reflect non-perfect NA61/SHINE acceptance in azimuthal angle.

In Fig. 1 the mean multiplicities of all charged particles $\langle N_{ch} \rangle$ are presented. The values are obtained in different transport models. Results for $\langle N_{ch} \rangle$ show that all models are in a good agreement in case experimental acceptance is applied, however, for a 4π and $|y| < 1$ rapidity range results start to slightly differ.

A. Scaled variance for particle number fluctuations

The scaled variances $\omega[X]$ are calculated for multiplicities of all charged N_{ch} , positively charged N_+ , and negatively charged N_- particles in different acceptance regions.

Although for charged particle multiplicity $\langle N_{ch} \rangle$ results of all models were quite in agreement, the values of scaled variance $\omega[X]$ differ and even show different behaviors that has to be explained.

In Fig. 2 the calculated values of ω as functions of $\sqrt{s_{NN}}$ are presented. On the top panel results for p+p inelastic collisions are shown. EPOS and UrQMD are in an approximate agreement with each other while HSD model produces smaller particle number fluctuations. We recall that the LUND string fragmentation model [32] is adopted for the description of the elementary p+p collisions in the (P)HSD approach. UrQMD and EPOS show strong growth of fluctuations when rapidity cut is applied that goes in contradiction with assumption that fluctuations get closer to the value of 1 in case some acceptance is applied (Eq. 5). UrQMD shows the highest growth in $|y| < 1$, while for EPOS fluctuations are slightly smaller and HSD gives the smallest fluctuations among above three models. However, if one studies fluctuations of particle number with $|y| < 1$ all three models show growth of scaled variance as compared to results in the full rapidity region.

For the Ar+Sc collisions in Fig. 2 (middle panel) picture changes. If for p+p collisions ω values produced by EPOS were between UrQMD and HSD results, then for Ar+Sc collisions EPOS gives the strongest fluctuations among all of the studied models. This is the result of fluctuations of participant number, however, the concept of participants is not strictly defined in the EPOS model.

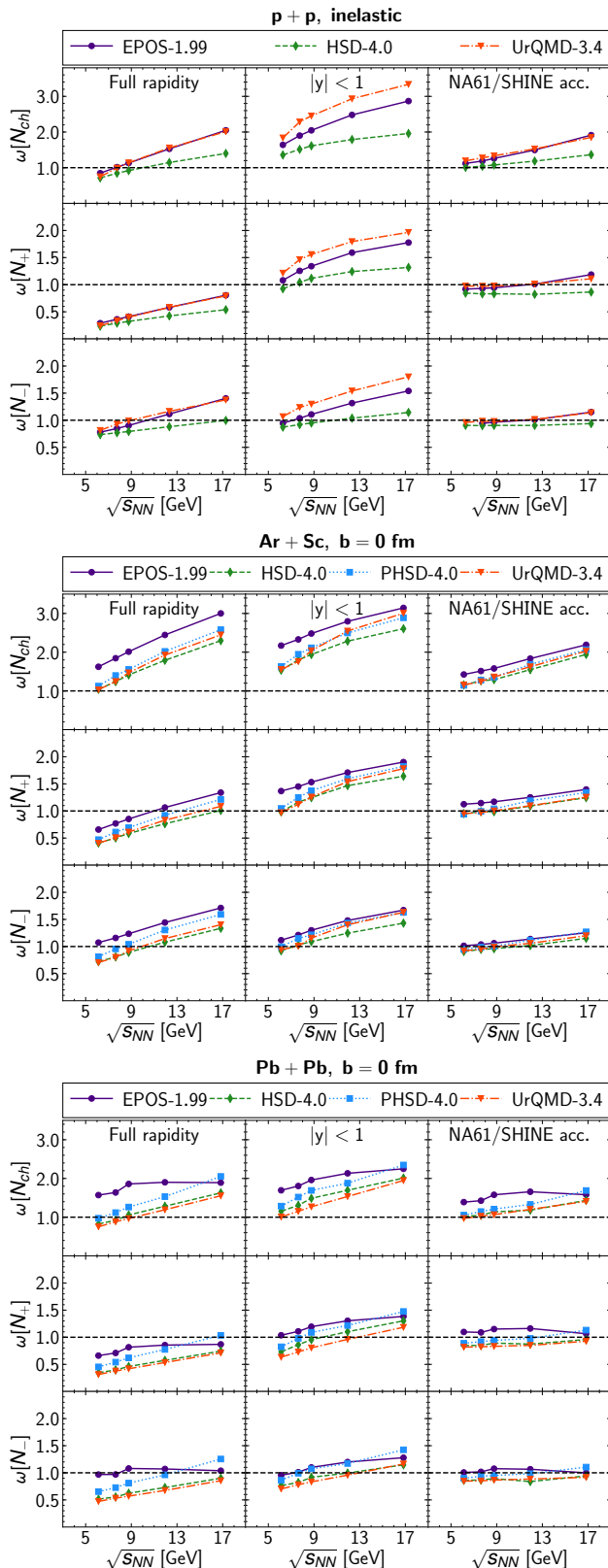


Figure 2: Comparison of EPOS (purple circles), HSD (green diamonds), PHSD (blue squares), and UrQMD (red triangles) results for scaled variance $\omega[X]$ of number of charged particles N_{ch} , number of positively charged particles N_+ and number of negatively charged particles N_- in inelastic p+p collisions (**top**), $b = 0$ fm Ar+Sc collisions (**middle**), and $b = 0$ fm Pb+Pb collisions (**bottom**) with different acceptance applied: full rapidity region (left), central rapidity region $|y| < 1$ (**center**) and NA61/SHINE acceptance (**right**).

In Ar+Sc results the rise of scaled variance ω is still present in case rapidity cut $|y| < 1$ is applied. However, that rise is not so strong as for p+p collisions and thus it indicates that system size plays a role in particle number fluctuations in central rapidity region. Charge conservation should take a dominant role in p+p collisions, since charged particles are only produced by pairs. In small systems as p+p is, there is not so much available energy as in large systems like created in A+A collisions and so production of particle-antiparticle pair takes large part of total energy. Because multiplicities in p+p collisions are not large and system evolution time is not enough to reach equilibrium, the produced particles are correlated as a result of the energy-momentum conservation. If charged particle is produced with transverse momenta p_T then there should be produced charged antiparticle with transverse momenta $-p_T$ – so transverse momenta of these particles are correlated. That could be the reason for the rise of particle number fluctuations in central rapidity region $|y| < 1$ since that region is dominated by particles with non-zero p_T .

In Pb+Pb collisions the behavior of scaled variance ω is not very different from Ar+Sc collisions. In Fig. 2 (bottom panel) the results for scaled variance ω of N_{ch} , N_+ , and N_- in Pb+Pb collisions simulated in studied models are presented. Still EPOS produces fluctuations that are stronger than in other models, but at top energies fluctuations stop to grow and then plateau is observed. In case the scaled variance with NA61/SHINE acceptance applied one sees that plateau is reached at energies $\sqrt{s_{NN}} = 9 \div 11$ GeV. The reason for this plateau in scaled variance ω is not clear.

B. Strongly intensive measures Δ and Σ

The strongly intensive measures – Δ and Σ are not dependent on system-size fluctuations and thus these quantities do not require complicated centrality selection. The $\Delta[K^+, \pi^+]$ as well as $\Sigma[K^+, \pi^+]$ were calculated using studied transport models. The values were obtained as in previous results in three acceptance regions: full acceptance, central rapidity region $|y| < 1$, and with NA61/SHINE acceptance applied. In Fig. 3 the all calculated values of Δ and Σ are presented. For p+p collisions all models produce values that are tightly located near value of 1. For Ar+Sc and Pb+Pb collisions models do not show so good agreement between each other, as for p+p. With the growth of system size the difference between studied models starts to increase, with non-trivial behavior for UrQMD and (P)HSD results.

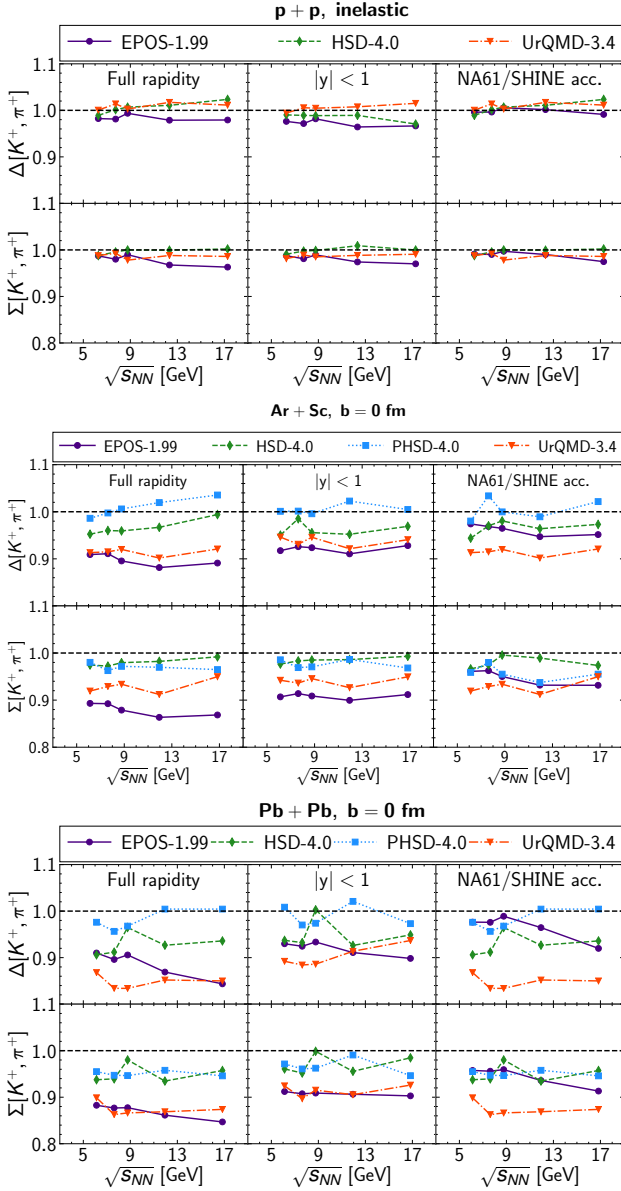


Figure 3: Strongly intensive measures $\Delta[K^+, \pi^+]$ and $\Sigma[K^+, \pi^+]$ in inelastic p+p collisions (**top**), $b = 0$ fm Ar+Sc collisions (**middle**), and $b = 0$ fm Pb+Pb collisions (**bottom**). Comparison of EPOS (purple circles), HSD (green diamonds), PHSD (blue squares) and UrQMD (red triangles) results with different acceptance applied: full rapidity region (**left**), central rapidity region $|y| < 1$ (**center**), and NA61/SHINE acceptance (**right**).

C. Scaled variance in different rapidity regions

In order to study the acceptance dependence of particle number fluctuations, the scaled variance ω has

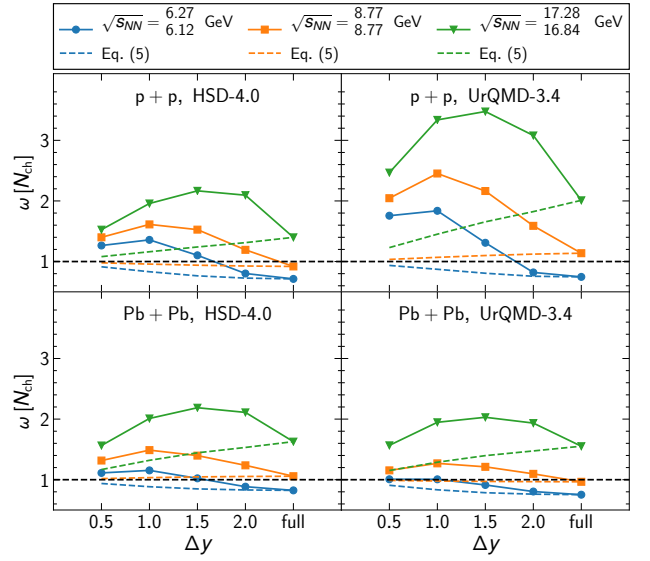


Figure 4: $\omega[N_{ch}]$ in inelastic p+p (**top**) and $b = 0$ fm Pb+Pb (**bottom**) collisions calculated in different rapidity regions within HSD (**left**) and UrQMD (**right**) models for different energies $\sqrt{s_{NN}}$ (upper numbers correspond to p+p collisions and lower numbers – to Pb+Pb). The predictions of Eq.5 are presented as dashed lines.

been calculated in different rapidity regions $|y| < \Delta y$. In Fig. 4 the scaled variances $\omega[N_{ch}]$ versus Δy are presented by solid lines. The dashed lines show the behavior which follows from Eq.5. According to Eq.5 the scaled variance ω should monotonously converge to the value of 1 while rapidity region Δy decreases to zero. However, Fig. 4 shows that $\omega[N_{ch}]$ has a non-monotonous dependence on Δy . Therefore, monotonous decrease of scaled variance according to Eq.5 appears to be in a contradiction with transport model results.

For p+p collisions, UrQMD shows much stronger fluctuations than HSD. That difference could be explained by the different particle production mechanisms in UrQMD and HSD. Namely, in HSD particle production is dominated by string fragmentation, while in UrQMD most of the particles are produced by resonance decays. Resonance decays result in uniform angular distribution of produced particles momenta, whereas string fragmentation takes place mostly along string direction so transverse mass m_T of produced particles is exponentially suppressed as $\exp(-bm_T^2/x)$, where b is the string model parameter and x is the energy-momentum fraction from the fragmenting string.

D. System size dependence and comparison with experimental data

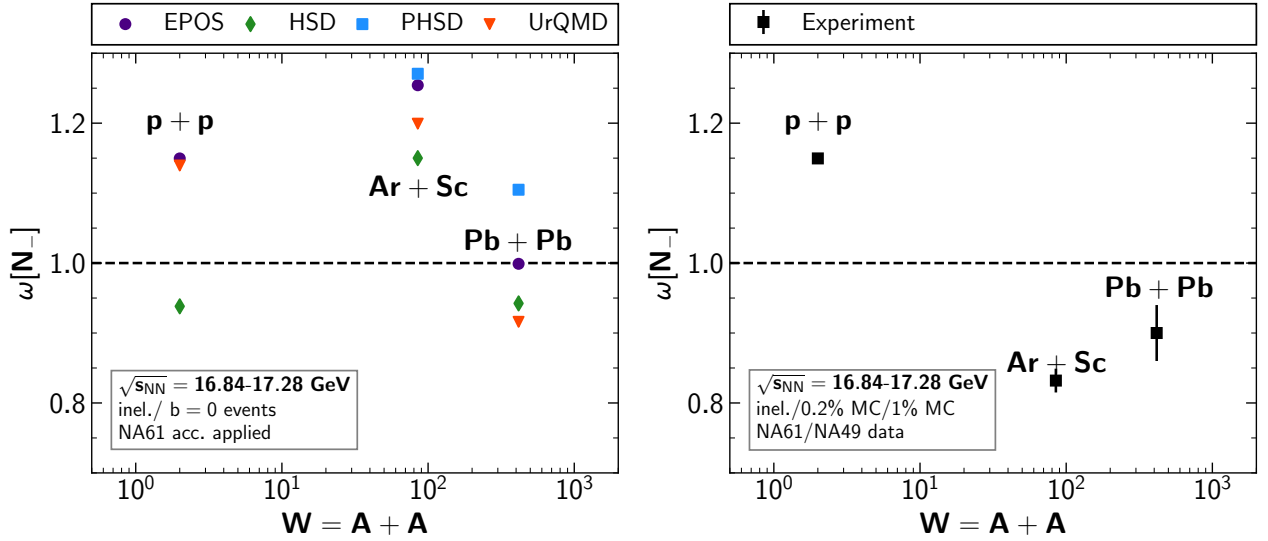


Figure 5: Scaled variance of multiplicity distribution of negatively charged particles N_- as function of system size (mass number $W=A+A$ of colliding system). **Left:** model results for inelastic proton-proton collisions and $b = 0$ fm A+A collisions with NA61/SHINE acceptance applied. **Right:** NA61/SHINE data for inelastic p+p collisions and Ar+Sc for 0-0.2% most central collisions, NA49 Pb+Pb collisions for 0-1% most central interactions.

Recently, the NA61/SHINE Collaboration presented the results for $\omega[N_-]$ in Ar+Sc collisions [17]. A non-trivial effect was observed – the $\omega[N_-]$ in Ar+Sc is much lower than in p+p collisions at the same $\sqrt{s_{NN}}$. These results contradict the wounded nucleon model, which, according to Eq.6, predicts scaled variance $\omega[X]$ in A+A collisions to be larger or equal (if $\omega_p[N_{part}] = 0$) than $\omega_{NN}[X]$.

In Fig. 5 the dependence of $\omega[N_-]$ on the system size calculated in different transport models is presented, and the experimental results from [17, 38] are shown for comparison¹. The UrQMD and EPOS models show a good agreement with experimental data on p+p collisions, while HSD underestimates $\omega[N_-]$.

For Ar+Sc results all models produce fluctuations that are essentially stronger than the ones observed in experiment. The deviation of calculated values from

data could be due to the very high centrality class selection at experiment for which $b = 0$ fm approximation might not be correct, see [17]. We have tested that selecting events with high number of participants in $b = 0$ fm Ar+Sc collisions in all models leads to decrease of $\omega[N_-]$ so discrepancy between the data and calculated values becomes smaller. These results are omitted in the present paper and are left for the future studies, since the large statistics should be collected and a proper correspondence between definition of participants and spectators in experiment and in calculations should be established to compute within the models the 0-0.2% most central data for rigorous comparison.

The $b = 0$ fm Pb+Pb collisions are a good approximation for the 0-1% most central events. HSD and UrQMD results are in satisfactory agreement with experimental data, while EPOS and PHSD give overestimated values for the scaled variance. In EPOS it is again the result of large participant number fluctuations in that model, in PHSD it is a result of ensemble averaging method implemented in the model where conserved quantities are conserved only on the average. The agreement between $b = 0$ fm HSD and UrQMD results with experimental values indicates that for large systems (that Pb+Pb is) the $b = 0$ fm collisions is a good approximation to the 0-1% ex-

¹ Please note, that NA49 acceptance for Pb+Pb point [38] was slightly smaller than the acceptance currently used by NA61/SHINE. In both cases $0 < y_\pi < y_{beam}$ rapidity range was used but in the NA49 analysis additional track cuts were used which reduced the mean multiplicity of negatively charged hadrons by 9% when compared to basic $0 < y_\pi < y_{beam}$ cut.

perimental collisions, this was previously studied in Ref. [39].

V. SUMMARY

All of the studied transport models do not show any signs of transition to deconfined phase in fluctuation measures. Although in the PHSD model the partonic degrees of freedom are present, and the horn in K^+/π^+ ratio is reproduced [36], still there is no non-monotonic behavior on particle number fluctuations as function of beam energy. However, some interesting properties are observed for scaled variances $\omega[X]$ as functions of the system size and applied acceptance. Namely, all transport models appear to be in contradiction with the often used formulae implementing the acceptance effects and connecting the fluctuations in A+A with those in p+p collisions. It is observed that, in contrast to Eq. (5), $\omega[X]$ depends non-monotonously on the size of the acceptance interval in the central rapidity region. One also sees that in the most central Ar+Sc and Pb+Pb collisions the scaled variance $\omega[N_-]$ is smaller than its value in inelastic p+p collisions at the same collision energy $\sqrt{s_{NN}}$. This result is in a contradiction with the model of independent sources (6).

Transport models with experimental acceptance of NA61/SHINE detectors applied, show that for Ar+Sc collisions fluctuations are larger than in p+p collisions, but for Pb+Pb scaled variance is smaller than in p+p and is very close to 1. The comparison with p+p experimental data (Fig. 5) shows that calculations within transport models are in agreement with the data for negatively charged particle number fluctua-

tions for p+p and Pb+Pb collisions. The underestimation of the $\omega[N_-]$ data for p+p by the HSD can be attributed to the lack of LUND string model adopted for the description of elementary collisions there. For $b = 0$ fm Ar+Sc collisions all models strongly overestimate the NA61/SHINE data for fluctuations in 0-0.2% most central events. Transport models give satisfactory description for $\omega[N_-]$ data measured by the NA49 Collaboration, only PHSD produces overestimated values. The notable discrepancy between transport models calculations and experimental data for Ar+Sc collisions is a subject for future studies.

VI. ACKNOWLEDGEMENTS

We are thankful to Larissa Bravina, Jan Steinheimer, Horst Stöcker, and Volodymyr Vovchenko for fruitful discussions. A.M. acknowledges the support by HGS-HIRe for FAIR, and Norwegian Centre for International Cooperation in Education, Grant No. CPEA-LT-2016/10094. The work of K.G. was partially supported by the National Science Center, Poland grant 2015/18/M/ST2/00125. The work of M.I.G. is supported by the Program of Fundamental Research of the Department of Physics and Astronomy of National Academy of Sciences of Ukraine, and by the Goal-Oriented Program of the National Academy of Sciences of Ukraine and the European Organization for Nuclear Research (CERN), Grant CO-1-3-2017. The work has been performed in the framework of COST Action CA15213 THOR. The computational resources have been provided by the LOEWE-CSC.

-
- [1] H. Heiselberg, Phys. Rept. **351**, 161 (2001) doi:10.1016/S0370-1573(00)00140-X [nucl-th/0003046].
- [2] S. Jeon and V. Koch, In *Hwa, R.C. (ed.) et al.: Quark gluon plasma* 430-490 [hep-ph/0304012].
- [3] M. Asakawa and M. Kitazawa, Prog. Part. Nucl. Phys. **90**, 299 (2016) doi:10.1016/j.ppnp.2016.04.002 [arXiv:1512.05038 [nucl-th]].
- [4] K. Werner, F. M. Liu and T. Pierog, Phys. Rev. C **74**, 044902 (2006) doi:10.1103/PhysRevC.74.044902 [hep-ph/0506232].
- [5] K. Werner, I. Karpenko, T. Pierog, M. Bleicher and K. Mikhailov, Phys. Rev. C **82**, 044904 (2010) doi:10.1103/PhysRevC.82.044904 [arXiv:1004.0805 [nucl-th]].
- [6] W. Cassing and E. L. Bratkovskaya, Phys. Rev. C **78**, 034919 (2008) doi:10.1103/PhysRevC.78.034919 [arXiv:0808.0022 [hep-ph]].
- [7] W. Cassing and E. L. Bratkovskaya, Nucl. Phys. A **831**, 215 (2009) doi:10.1016/j.nuclphysa.2009.09.007 [arXiv:0907.5331 [nucl-th]].
- [8] S. A. Bass *et al.*, Prog. Part. Nucl. Phys. **41**, 255 (1998) [Prog. Part. Nucl. Phys. **41**, 225 (1998)] doi:10.1016/S0146-6410(98)00058-1 [nucl-th/9803035].
- [9] M. Bleicher *et al.*, J. Phys. G **25**, 1859 (1999) doi:10.1088/0954-3899/25/9/308 [hep-ph/9909407].
- [10] V. P. Konchakovski, S. Haussler, M. I. Gorenstein, E. L. Bratkovskaya, M. Bleicher and H. Stoecker, Phys. Rev. C **73**, 034902 (2006) doi:10.1103/PhysRevC.73.034902 [nucl-th/0511083].
- [11] V. P. Konchakovski, M. I. Gorenstein,

- E. L. Bratkovskaya and H. Stoecker, Phys. Rev. C **74**, 064911 (2006) doi:10.1103/PhysRevC.74.064911 [nucl-th/0606047].
- [12] M. I. Gorenstein, M. Hauer, V. P. Konchakovski and E. L. Bratkovskaya, Phys. Rev. C **79**, 024907 (2009) doi:10.1103/PhysRevC.79.024907 [arXiv:0811.3089 [nucl-th]].
- [13] V. P. Konchakovski, M. I. Gorenstein, E. L. Bratkovskaya and W. Greiner, J. Phys. G **37**, 073101 (2010) doi:10.1088/0954-3899/37/7/073101 [arXiv:1001.3085 [nucl-th]].
- [14] V. V. Begun, V. P. Konchakovski, M. I. Gorenstein and E. Bratkovskaya, J. Phys. G **40**, 045109 (2013) doi:10.1088/0954-3899/40/4/045109 [arXiv:1205.6809 [nucl-th]].
- [15] V. Y. Vovchenko, D. V. Anchishkin and M. I. Gorenstein, Phys. Rev. C **90**, no. 2, 024916 (2014) doi:10.1103/PhysRevC.90.024916 [arXiv:1407.0629 [nucl-th]].
- [16] J. Steinheimer, V. Vovchenko, J. Aichelin, M. Bleicher and H. Stöcker, arXiv:1608.03737 [nucl-th].
- [17] A. Seryakov [NA61/SHINE Collaboration], Acta Phys. Polon. B Proc. Suppl. **10**, 723 (2017) [arXiv:1704.00751 [hep-ex]].
- [18] N. Antoniou *et al.* [NA49-future Collaboration], CERN-SPSC-2006-034, CERN-SPSC-P-330.
- [19] N. Abgrall *et al.* [NA61 Collaboration], JINST **9**, P06005 (2014) doi:10.1088/1748-0221/9/06/P06005 [arXiv:1401.4699 [physics.ins-det]].
- [20] A. Seryakov, private communication
- [21] M. I. Gorenstein and M. Gazdzicki, Phys. Rev. C **84**, 014904 (2011) doi:10.1103/PhysRevC.84.014904 [arXiv:1101.4865 [nucl-th]].
- [22] V. V. Begun, M. I. Gorenstein and O. S. Zozulya, Phys. Rev. C **72**, 014902 (2005) doi:10.1103/PhysRevC.72.014902 [nucl-th/0411003].
- [23] A. Bialas, M. Bleszynski and W. Czyz, Nucl. Phys. B **111**, 461 (1976) doi:10.1016/0550-3213(76)90329-1
- [24] H. J. Drescher, M. Hladik, S. Ostapchenko, T. Pierog and K. Werner, Phys. Rept. **350**, 93 (2001) doi:10.1016/S0370-1573(00)00122-8 [hep-ph/0007198].
- [25] E. L. Bratkovskaya, W. Cassing, V. P. Konchakovski and O. Linnyk, Nucl. Phys. A **856**, 162 (2011) doi:10.1016/j.nuclphysa.2011.03.003 [arXiv:1101.5793 [nucl-th]].
- [26] W. Cassing, Eur. Phys. J. ST **168**, 3 (2009) doi:10.1140/epjst/e2009-00959-x [arXiv:0808.0715 [nucl-th]].
- [27] L. P. Kadanoff and G. Baym, *Quantum Statistical Mechanics*, Benjamin, New York, 1962.
- [28] W. Cassing and E. L. Bratkovskaya, Phys. Rept. **308**, 65 (1999) doi:10.1016/S0370-1573(98)00028-3
- [29] W. Cassing, E. L. Bratkovskaya and S. Juchem, Nucl. Phys. A **674**, 249 (2000) doi:10.1016/S0375-9474(00)00163-9 [nucl-th/0001024].
- [30] H. Berrehrah, E. Bratkovskaya, T. Steinert and W. Cassing, Int. J. Mod. Phys. E **25**, no. 07, 1642003 (2016) doi:10.1142/S0218301316420039 [arXiv:1605.02371 [hep-ph]].
- [31] V. Ozvenchuk, O. Linnyk, M. I. Gorenstein, E. L. Bratkovskaya and W. Cassing, Phys. Rev. C **87**, no. 6, 064903 (2013) doi:10.1103/PhysRevC.87.064903 [arXiv:1212.5393 [hep-ph]].
- [32] B. Andersson, G. Gustafson and H. Pi, Z. Phys. C **57**, 485 (1993) doi:10.1007/BF01474343
- [33] V. P. Konchakovski, W. Cassing and V. D. Toneev, J. Phys. G **42**, no. 5, 055106 (2015) doi:10.1088/0954-3899/42/5/055106 [arXiv:1411.5534 [nucl-th]].
- [34] V. P. Konchakovski, E. L. Bratkovskaya, W. Cassing, V. D. Toneev and V. Voronyuk, Phys. Rev. C **85**, 011902 (2012) doi:10.1103/PhysRevC.85.011902 [arXiv:1109.3039 [nucl-th]].
- [35] O. Linnyk, E. L. Bratkovskaya and W. Cassing, Prog. Part. Nucl. Phys. **87**, 50 (2016) doi:10.1016/j.pnpnp.2015.12.003 [arXiv:1512.08126 [nucl-th]].
- [36] A. Palmese, W. Cassing, E. Seifert, T. Steinert, P. Moreau and E. L. Bratkovskaya, Phys. Rev. C **94**, no. 4, 044912 (2016) doi:10.1103/PhysRevC.94.044912 [arXiv:1607.04073 [nucl-th]].
- [37] Acceptance maps used in the paper: “Multiplicity and transverse momentum fluctuations in proton-proton interactions,” <https://edms.cern.ch/document/1549298/1>
- [38] C. Alt *et al.* [NA49 Collaboration], Phys. Rev. C **78**, 034914 (2008) doi:10.1103/PhysRevC.78.034914 [arXiv:0712.3216 [nucl-ex]].
- [39] V. P. Konchakovski, B. Lungwitz, M. I. Gorenstein and E. L. Bratkovskaya, Phys. Rev. C **78**, 024906 (2008) doi:10.1103/PhysRevC.78.024906 [arXiv:0712.2044 [nucl-th]].